Spring 2020

Optimization of Vehicle to Grid System in a Power System With Unit Commitment

Charles Uko

OPTIMIZATION OF VEHICLE TO GRID SYSTEM IN A POWER SYSTEM WITH UNIT COMMITMENT

by

Charles Uko

Bachelor of Science
Kwame Nkrumah University of Science and Technology, 2013

Submitted in Partial Fulfillment of the Requirements

For the Degree of Master of Science in

Electrical Engineering

College of Engineering and Computing

University of South Carolina

2020

Accepted by:

Ona Egbue, Director of Thesis

Enrico Santi, Reader

Zafer Gurdal, Reader

Cheryl L. Addy, Vice Provost and Dean of the Graduate School

DEDICATION

This Thesis is dedicated to God almighty for the gift of life, strength, and wisdom to be able to undertake this master's degree program successfully. I would also like to thank my parents and my siblings for their love, support, and encouragement that inspired me to complete this research.

ACKNOWLEDGMENTS

I wish to express my deepest gratitude to my Advisor, Dr. Ona Egbue, whose support made this research and thesis possible. Special thanks goes to the Energy, Power, Control and Network (EPCN) program of the National Science Foundation under grant number 171167 for supporting this project. I would also love to extend my sincerest appreciation to the other members of my research team Dr. Naidu, and Charles Anyim, for their support and being a part of this journey. I would also love to thank my committee members Dr. Enrico Santi and Dr. Zafer Gurdal, for taking time out of their very busy schedule to oversee my work.

ABSTRACT

This thesis provides a comprehensive overview and analysis of using plug-in electric vehicles (PEVs) in solving the unit commitment problem. PEVs are becoming more attractive and a rapid replacement of conventional fuel vehicles due to their environmental-friendly operation. Through collective control by an aggregator, PEVs batteries can also provide ancillary services such as load leveling and frequency regulation to improve the quality of power supplied in the power grid and reduce the cost of power generation. This study presents the modeling, simulation, and analysis of a vehicle-to-grid (V2G) system connected to a smart power grid. The model considers different penetration levels of PEVs in a system and investigates the economic and technical effects of using PEVs to support the grid. The model is tested using an IEEE 24 bus network to verify the effects that PEVs penetration has on generation cost in power systems. A comparison has been made between a system without V2G and a system with V2G to produce justification for the role that V2G can play in solving the unit commitment problem. The results of this study show that the optimal scheduling of PEVs was effective in flattening the load profile through valley filling and peak load reduction.

TABLE OF CONTENTS

LIST OF TABLES

LIST OF FIGURES

LIST OF SYMBOLS

Index:

b	Index of buses.
g	Index of thermal units.
i	Index of plug-in electric vehicles.
t	Index of hours.

Parameters:

a_g, b_g, c_g	Cost coefficients of generation set g.
arr^i_{time}	Arrival time of vehicle i.
Bat^i_{cap}	Battery capacity of vehicle i.
$Cdeg_{i,t}$	Degradation cost of PEV I at time t.
$cycle_i$	Sum of cycles of vehicle i.
dep^i_{time}	Departure time of vehicle i.
δ_b	Voltage angle of bus b.
δ_n	Voltage angle of bus n.
$DT_{g,0}$	Periods thermal unit has been off before the start of the optimization.
$Load_{b,t}$	Non-EV load demand on bus b at time t.
$minUT$	Minimum up-time constraint for generator.
$Msoc^i$	Minimum required state of charge of vehicle i.
η_{chg}	Charging efficiency.

η_{dch}	Discharging efficiency.
$P_{g,t}$	Operating power of generator g at time t.
P_g^{max}	Maximum operating power limit of generator g.
P_g^{min}	Minimum operating power limit of generator g.
P_{nb}	Active power flow between buses n and b.
P_{total}^t	Total power charged during period t.
$RampDown_g$	Ramp-down power limit of generator g.
$RampUp_g$	Ramp-up power limit of generator g.

Variables:

$C_{chg}^{i,t}$	Charging power of vehicle i at time t.
$C_{dch}^{i,t}$	Charging power of vehicle i at time t.
$cend_{i,t}$	Binary variable that indicates the end of a discharging cycle.
$charge_{i,t}$	Binary variable that indicates an increase in SOC of PEV i.
$cstart_{i,t}$	Binary variable that indicates start of a discharging cycle.
$discharge_{i,t}$	Binary variable that indicates when there is a decrease in SOC of PEV i.
$I_{chg}^{i,t}$	Binary variable representing the charging status of vehicle i at time t.
$I_{dch}^{i,t}$	Binary variable representing the discharging status of vehicle i at time t.
$soc^{i,t}$	State of charge of vehicle i at time t.
$stable_{i,t}$	Binary variable that indicates when no activity takes place.
$u_{g,t}$	Binary variable representing operation state of generator g at time t.
$y_{g,t}$	Binary variable representing start-up state of generator g at time t.
$z_{g,t}$	Binary variable representing shut-down state of generator g at time t.

LIST OF ABBREVIATIONS

AC	Alternating Current
DC	Direct Current
DOD	Depth of Discharge
EV	Electric Vehicle
EVSE	Electric Vehicle Service Equipment
G2V	Grid-to-Vehicle
GAMS	General Algebraic Modeling System
kW	Kilowatt
kWh	Kilowatt-hour
MILP	Mixed Integer Linear Programming
NHTS	National Household Travel Survey
NREL	National Renewable Energy Laboratory
PEV	Plug-in Electric Vehicle
PJM	Pennsylvania New Jersey Maryland Interconnection
RTP	Real-Time Pricing
SAE	Society of Automotive Engineers
SOC	State of Charge
TOU	Time of Use
UC	Unit Commitment
V2G	Vehicle-to-Grid

CHAPTER 1

INTRODUCTION

PEVs are becoming more attractive and a rapid replacement of conventional fuel vehicles due to their environmental-friendly operation. Analysis of the electric vehicle index conducted by EV-Volumes, a leading database of electric vehicles shows that the global PEV population is growing exponentially [1]. Electric vehicle sales grew to more than two million units globally in 2018, and there is potential for increased growth rate as the electric vehicle population is just a fraction of the overall light-vehicle market. This is shown by research conducted by Mckinsey & Company [2] where the penetration rate of light electric vehicles among overall light-vehicles in 2018 was found to be 3.9%, 1.8% and 2.1% for China, the European Union, and the United States respectively.

Despite the benefits of PEVs, the high penetration of PEVs into the power system can lead to an undesirable impact on the power system's quality of electricity if not adequately managed [3]. A potential solution to this will be the expansion of the power grid infrastructure such as transmission line and transformer capacities. Still, issues such as land availability, the environmental impact of building more infrastructure, and legal issues make this an expensive and time-intensive option. An easier solution to this problem will be for the smart grid network to control the charging demand of PEVs to reduce any negative impact that PEVs might have on the power grid. Controlling the charging of PEVs will also ensure that both the desires of the PEV drivers and the power grid needs are met.

Through collective control by an aggregator, PEVs batteries can also provide ancillary services such as load leveling and frequency regulation to improve the quality of the power supplied in the power grid. The control will be ensured through optimal scheduling that considers different technical aspects of the system and using the PEVs batteries to offset any of the power system abnormalities. PEVs batteries are also used in power systems with a considerable penetration of renewable energy resources, where the intermittent availability of power supply is a common occurrence. PEVs can control their energy demand, and PEV batteries can also act as back-up power supplies to maintain grid stability. The higher the penetration of PEVs in the system, the higher the available capacity of quick energy for cycling and instant power delivery to the power grid hence turning this high penetration into an advantage for the power system health.

1.1 RESEARCH GOAL AND MAIN CONTRIBUTION OF THESIS

This research presents the modeling, simulation, and analysis of a vehicle-to-grid (V2G) system connected to a smart power grid. The model considers different penetration levels of PEVs in a system and investigates the economic and technical effects of using PEVs to support the power grid.

Specific objectives of this thesis include:

1.) To incorporate the travel behavior of individual drivers into V2G optimization and the unit commitment problem.
2.) Analysis of the effects of using PEVs in solving the unit commitment problem.
3.) Analysis of the cost implications charging and discharging has on the battery life of PEVs.

The model is tested using an IEEE 24 bus network to verify the effects that PEVs penetration has on generation cost in power systems. The main contribution of this thesis is the analysis and presentation of results of using PEVs to solve the unit commitment problem for the given case study. The results of this study show that the optimal scheduling of PEVs was effective in flattening the load profile through valley filling and peak load reduction.

1.2 THESIS STRUCTURE

This thesis is organized into five main chapters: The first chapter presents the introduction and overview of the study, including research objectives. The second chapter provides a literature survey of electric vehicles used in the unit commitment problem in a power grid. It also reviews studies on the issues associated with using PEVs to support the unit commitment problem. The third chapter provides the classification of the PEVs, and their characteristics such as travel behavior, SOC demand, battery capacity and further discusses the methodology used in this study for the implementation of the optimization model. It also discusses the tools used to carry out the modeling and the various solvers used. The fourth chapter presents the results of solving the unit commitment model with the PEV loads. The results are analyzed and displayed in figures to assist with understanding. The fifth and final chapter presents the conclusion of the study. In this chapter, future studies and potential improvements to be made on the existing model are also proposed.

CHAPTER 2

LITERATURE REVIEW

In this chapter, a detailed overview of research work related to V2G is presented. This chapter will discuss the V2G concept, and the collective use of PEVs to curb or control issues such as grid failure and also provide a look into the challenges facing V2G technology.

2.1 VEHICLE TO GRID TECHNOLOGY

In vehicle to grid technology, the basic idea is for vehicles to provide support to the grid while they are plugged into the power grid. Early studies on V2G such as that conducted by Kempton, states the primary requirements for vehicles participating in V2G [4]. These include: (1) Connection to the power grid, usually as a charging station or unit (2) Means of control or communication with the grid operator (3) Controls and metering on the vehicle. Vehicle types that can participate in V2G include battery EVs, fuel cell EVs and plug-in hybrid EVs. Battery EVs are electric vehicles that depend entirely on the stored energy in the vehicle's batteries for power. They can also be referred to as full electric or all-electric. Their mechanism can include a regenerative braking system that can be used to charge the vehicle battery while braking is taking place. Fuel cell EVs are powered by hydrogen and can store the energy in a battery. Even though the refueling time of fuel cell EVs is comparable to conventional ICEs and faster than that of battery EVs, a report by the National Renewable Energy Laboratory shows that hydrogen stations are expensive and capital intensive [5]. Plug-in hybrid EVs are powered by both a battery and an internal combustion engine (ICE). For our study, we will be limiting the vehicle types in our simulation to battery EVs.

2.2 CLASSIFICATION OF PEV CHARGERS

EV chargers can be classified based on different types of criteria: The table below shows the classification criteria and the various options [6].

Table 2.1 Classification of PEV chargers

Classification type	Options
Topology	Dedicated or integrated
Location	On-board or Off-board
Connection type	Conductive, Inductive, or Mechanical
Electrical waveform	AC or DC
The direction of power flow	Unidirectional or Bidirectional

The Society of Automotive Engineers (SAE) further classified PEV chargers into level 1, level 2, and DC fast chargers. The table below shows the different charger types and their charging power [7].

Table 2.2 Charging power levels for PEV chargers

EVSE type	Power Supply	Charging power	Approximate charging time for a 24kWh battery
AC charging station: Level 1 residential	120/230 VAC and 12 A to 16 A (single phase)	~1.44 kW to ~1.92 kW	~17 hours
AC charging station: Level 2 commercial	208/~240 VAC and 15 A to ~80 A (single/split phase)	~3.1 kW to ~19.2 kW	~8 hours
DC charging station: Level 3 fast chargers	300 to 600 VDC and max 400 A (polyphase)	From 120 kW up to 240 kW	~ 30 minutes

The level 2 charger has been chosen for the simulation in this thesis.

2.3 UNIDIRECTIONAL AND BIDIRECTIONAL CHARGING

There are two ways in which V2G can be applied, namely, unidirectional and bidirectional. In unidirectional V2G, the power flows in only one direction from the grid into the vehicle. Unidirectional V2G has the following benefits such as reducing emission, preventing grid overloading, maximizing profit and being inexpensive to implement. According to the National Renewable Energy Laboratory, most PEV charging stations and EVs are designed for unidirectional operation and several studies have researched unidirectional V2G [8]. A study by Sortomme et al. [9] proposed an aggregator profit maximization algorithm, which is a unidirectional regulation. Their algorithm was tested using simulation for the Pacific Northwest system with a hypothetical group of commuters. The results from their simulation showed that the optimized algorithms provided significant benefits to all participants in the system. Customers were able to minimize their charging cost and utility was able to improve the power system operation.

Another study by Sekyung et al. [10] proposed an algorithm to solve the optimization problem related to frequency regulation. This study considered a unidirectional V2G approach where regulation signals were sent to the vehicles in the grid to carry out charging in the most optimal schedule. An optimal charging control and regulation was achieved by considering constraints such as the energy capacity of the battery and weight functions were employed to reflect the energy constraint. The optimality of their model was verified by the results of their simulation. Another example of unidirectional V2G implementation is by Wang et al. [11]. They proposed a modeling framework for the maximization of revenues in a real-world demand response market in California. The objective of maximizing revenues was achieved using a mixed-integer programming approach and unidirectional PEV to grid interactions.

Bidirectional V2G allows for the flow of power in both directions. Active power can be transferred back and forth between the charger and the power grid. This mode of V2G has been shown to have a lot of economic benefits because the power grid can take advantage of the collective vast energy reserves of PEV batteries to support the grid, unlike the unidirectional charging where only the charging power and speed is controlled

[12]. Other services that can be provided by bidirectional charging include: peak shaving, reduction of power grid losses, power grid failure recovery, maximization of profit, minimization of emissions, valley filling, frequency, and voltage regulation [13]. Although bidirectional charging has all these attractive benefits, it is also important to note that it comes with drawbacks such as having high investment cost compared to unidirectional stations, requiring complicated hardware installation to support bidirectional power flow, battery degradation issues and social barriers [14]. There is a rise in the number of studies and proposed optimization models for bidirectional V2G because of the numerous benefits associated with bidirectional V2G. A study by Hashemi et al. [15] implements a centralized control method where two-way communication links are used to send and receive control signals on a second-by-second basis. Results from their study show that V2G enabled EVs were able to provide fast and accurate responses in a time of less than 5 seconds and accuracy response of about 98%.

Hajizadeh et al. [16] proposed an optimized approach to coordinate the bidirectional charging of PEVs to reduce power losses and improve the average voltage quality of feeders. Their algorithm used maximum sensitivity selection to achieve its objectives. The model was tested using an actual distribution network, and the results show that the speed and performance of the maximum sensitivity selection method was acceptable for a real-time application.

Huang et al. [17] proposed a multi-objective optimal strategy for coordinating the charging and discharging of EVs. An advanced genetic algorithm with a preservation policy was used to carry out the optimization of the process while considering measures such as the time of use (TOU) alongside the reactive compensation of energy storage devices. The model by Huang was demonstrated on an IEEE 33-node test case, and the results show that the optimal coordination of PEV charging and discharging helped to achieve power balance and mitigated power loss.

Bitencourt et al. [18] developed a model using MATLAB/ Simulink and linear programming technique to carry out the coordination of charging at the distribution transformer level. Their model used different pricing signals, such as time-of-use pricing and real-time pricing (RTP). Results showed that their model was effective in providing peak shaving for distribution transformers. RTP also showed better results in the optimal scheduling, and TOU pricing was able to shift the demand peak to a different time of the day.

2.4 V2G AND UNIT COMMITMENT

In this subchapter, we review studies that have applied V2G to solving the unit commitment problem. Hosseini et al. [19] proposed the use of V2G in a security-constrained unit commitment problem. Their problem was formulated as a mixed-integer linear problem and solved using GAMS software. They considered constraints such as the spinning reserve, generating capacity, power flow in the transmission lines, ramp rates, minimum up and downtime. Two scenarios were tested by first considering the system without V2G and with V2G. Their method was applied to the IEEE 6 bus, and 33 bus systems and their proposed model was useful in reducing the hourly operating cost. It was also helpful to the network operator for specifying the optimal number of vehicles needed to implement V2G for each hour.

Pan et al. [20] proposed a model to solve a stochastic security constraint unit commitment problem. The focus of their study was on the correlation of electric vehicles driving information to the result of the unit commitment optimization problem using V2G. The copula function was employed to generate the relevant vehicle driving data for the types of PEV used in their simulation. Their problem was solved using CPLEX, and results showed that there was a correlation between the PEV driving behavior and the use of V2G for solving the unit commitment problem. They concluded that it was therefore useful to study the travel behavior of participating vehicles to achieve the best schedules for the V2G dispatch.

Sadeghian et al. [21] examined a power system that utilized combined heat and power (CHP) units and PEVs in addition to conventional thermal generating units to reduce the generation cost of the power system. Their simulation was run for a total number of 50000 PEVs aggregated from various smart parking lots in the system. Although V2G was used here to solve the unit commitment problem, all the PEVs used were assumed to have the same parameters of the maximum battery capacity of 25kWh, an average battery capacity of 15 kWh and minimum battery capacity of 10 kWh. Results from their study show that the use of PEVs in the unit commitment problem was effective in the reduction of the system operation cost. The PEVs were able to provide additional reserve capacity and also eliminated the need for small, expensive units in the power systems. Cao et al. [22] introduced a novel multi-objective security-constrained unit commitment model that considered wind power and V2G. The wind forecasting was improved through the use of a fuzzy chance-constrained program, and game theory was used to formulate the PEVs scheduling. Their simulation was conducted on the IEEE 24-bus system, and results show that their proposed model was effective in achieving peak load shifting, reducing energy cost and reducing the PEV owner’s electric charges.

Yang et al. [23] introduced a binary symmetric based hybrid meta-heuristic method for solving a mixed-integer unit commitment problem with significant penetration of PEVs. Their proposed model combined the advantages of binary symmetric particle swarm optimization (PSO), self-adaptive differential evolution (SaDE), and lambda iteration method. Their study investigated a 10 unit power system with 50,000 plug-in electric vehicles and also considered unidirectional and bidirectional operation modes. The results of their research show that the use of V2G as flexible energy storage was effective in remarkably reducing the economic cost of the system.

Azari et al. [24] studied the effect of V2G on the operation cost and locational marginal price (LMP) on an IEEE 6 bus system. Their unit commitment optimization problem was formulated as the mixed-integer linear program (MILP) approach. The result of their simulation shows that the presence of electric vehicles resulted in increased system security. The ability of the electric vehicle load demand to be delayed to a later period was able to prevent the use of expensive units to generate power thus reducing the line congestion and decreasing the LMP. A study by Kumar et al. [25] proposed a population based metaheuristics algorithm known as the quasi oppositional water wave optimization (QOWWO) algorithm to solve the unit commitment problem. They investigated the impacts of PHEVs on an IEEE 10-unit test system over 24 hours, and their results show that total cost and emissions in the system reduced when PHEVs were integrated into the system. Another conclusion from their study was on the effective performance of the QOWWO algorithm compared to standard water wave optimization and other heuristic algorithms. Liu et al. [26] proposed a multi-objective security-constrained unit commitment model with wind power and V2G penetration. The objectives of their proposed model were to minimize the total cost of operation and mitigate pollutant emissions. The fuzzy chance-constrained program was adopted to handle the uncertainly in the system when considering the intermittent nature of wind power. The results of their study show that the model was effective in shifting power demands from periods of high demand to periods where wind power is abundant, thus reducing the stress on the available power supply. Maghsudlu and Sirus [27] considered a system with electric vehicles and photovoltaic sources in solving the unit commitment problem. The Monte Carlo optimization algorithm was used to handle the uncertain outputs of the solar power source, and a meta-heuristic Cuckoo search algorithm was used to solve the problem, which was tested on an IEEE 10-unit test system. The results of their simulation show that the use of PEVs led to a decrease in the total cost of power generation in the system.

CHAPTER 3

METHODOLOGY

In this chapter, the models and methodology in which the research is conducted are presented. This includes the generation of the driving profile for the vehicles used in the simulation, the load profile, and the mathematical formulation of the unit commitment problem.

Offline scheduling is the optimization method used in this study. In comparison to online scheduling models, optimization in offline scheduling is carried out using complete information of parameters used for formulation of the problem. An example of offline scheduling is the classical day-ahead scheduling problem for a power system where the information such as the load demand profile is available and used to carry out the scheduling of generation. For online scheduling, the load demand profile is not known ahead of time and it is determined at each period that the optimization is being conducted. In our research, we assume that information such as the arrival and departure time of the PEVs are known ahead of time. The assumptions of the arrival and departure time are extrapolated based on the National Household Travel Survey (NHTS) historical travel data.

3.1 DRIVER PROFILE

In this subchapter, the travel pattern of drivers is presented. It is essential to study the PEV agents' behavior because it has a significant impact on the distribution network and the utilization of the charging infrastructure [28]. Other information, such as the vehicle's physical properties used in modeling the problem is also considered. For ease of modeling, a discrete-time system is used to approximate the continuous-time used for our simulation. A total of 48 intervals of 1 hour each is used for the simulation of 2 days. The second day was added to ensure that the departure time of vehicles that arrived late the first day and couldn't complete charging at the end of the day could still be determined the next day. Information on the vehicles' physical properties was obtained from www.fueleconomy.gov, the official US government source for fuel economy information [29]. For the travel pattern, data from the National Household travel survey (NHTS) was used to model travel behavior [30]. Attributes such as travel speed, average commute distance to several destinations, and dwell time at each destination were inferred from data obtained from NHTS.

The travel pattern of 20,000 vehicles from the trip data set was analyzed, and the arrival time distribution for the vehicles was fitted using the distribution fitter app on MATLAB. It is assumed in our study that the aggregator considers PEVs at work, school, daycare, religious, shopping and leisure activities. Figure 3.1 below shows the arrival time distribution of vehicles for the locations mentioned above. The normal and non-parametric distribution of the arrival times are also included in the curve. From figure 3.1 below, it can be observed that the arrival time data for this study is not normally distributed and more closely follows a non-parametric distribution. The time distribution used for this study will be based on the fitting shown by the histogram in figure 3.1.

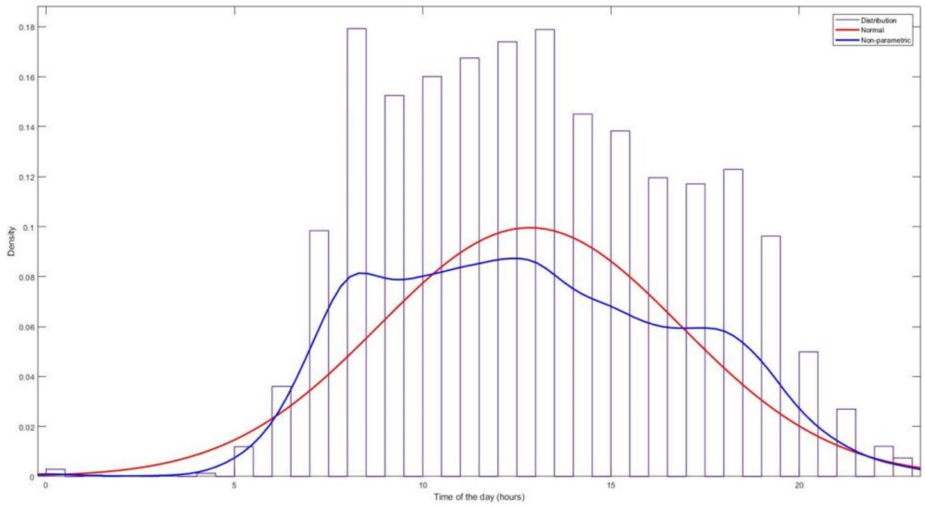

Figure 3.1 Distribution of arrival time for vehicles to locations

The dwell time, which is the time the vehicle spends at the parking lot, was also obtained from the NHTS trips dataset. Figure 3.2 below shows the distribution of vehicles dwell times at the destination. The time for the vehicles' departure was estimated as the sum of the arrival time and the dwell time.

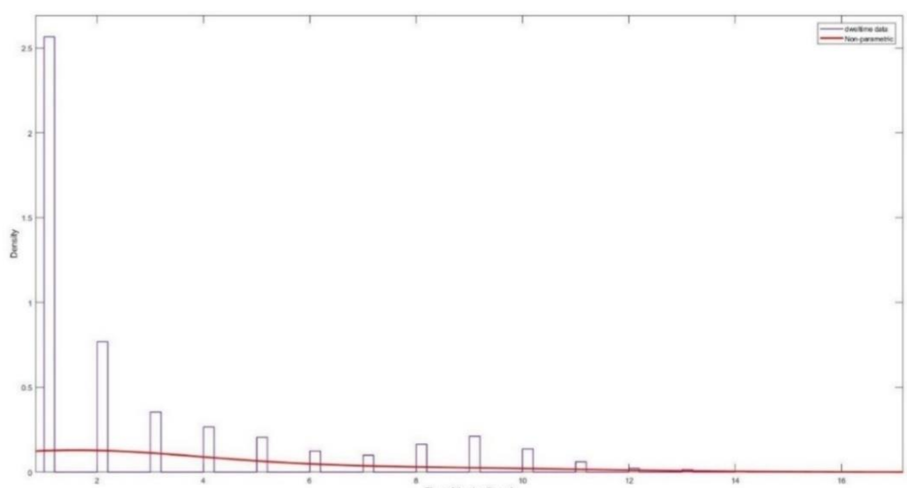

Figure 3.2 Distribution of dwell time for vehicles

The types of vehicles used in the study are generated based on the sales distribution of PEVs in the market obtained from EV-volumes [1].

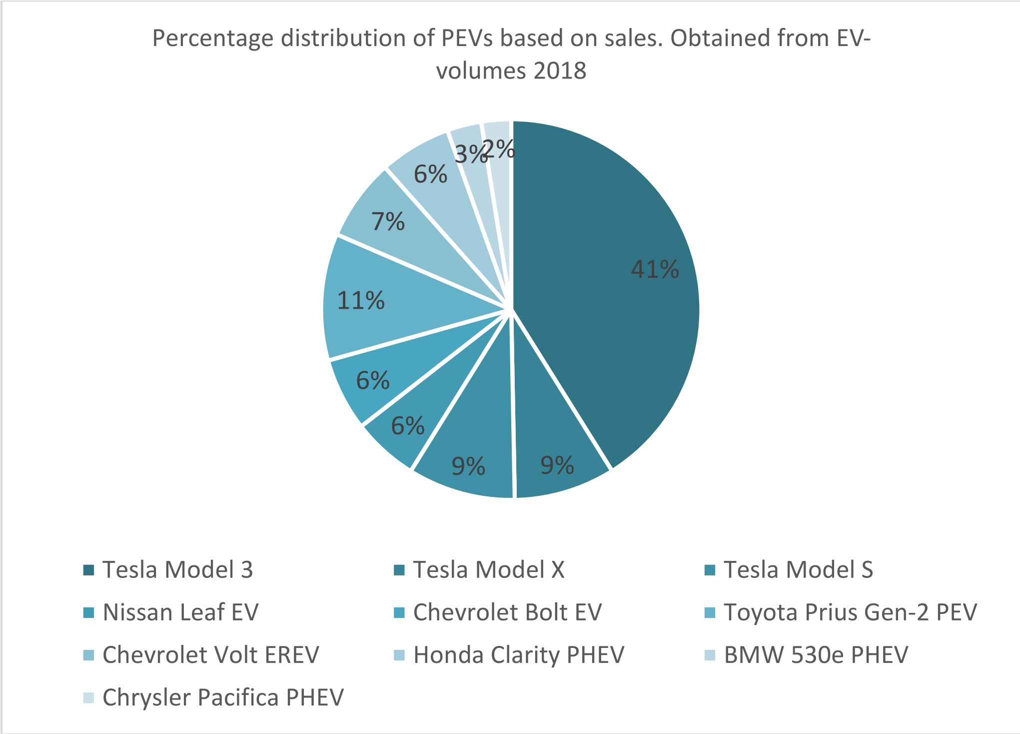

Figure 3.3 Distribution of electric vehicles based on sales.

Table 3.1: Properties of vehicles obtained from manufacturer's websites

EV brand	Battery Capacity(kWh)	Efficiency (Miles/kWh)
Tesla Model 3	50	3.7
Tesla Model X	75	2.5
Tesla Model S	75	2.86
Nissan Leaf EV	40	3.33
Chevrolet Bolt EV	60	3.57
Toyota Prius Gen-2 PEV	24	3.45
Chevrolet Volt EREV	30	3.23

Honda Clarity PHEV	25	3.33
BMW 530e PHEV	23	2.17
Chrysler Pacifica PHEV	35	2.45

3.2 MATHEMATICAL FORMULATION OF THE UNIT COMMITMENT PROBLEM

In this subchapter, the unit commitment problem is introduced. The proposed problem presented is a 24-bus system with ten different generators. Unit commitment in power system management is the operation and optimal planning of generation facilities to minimize the production costs of the system while considering factors like the ramp rates, and the operational limits of each generating unit. Unlike the economic dispatch problem, which only considers the fuel cost required to generate the power profile that each generating unit produces, the unit commitment problem considers three main cost components, which are the fuel costs, start-up cost, and shut-down costs of the generators in the system. This is a more complicated problem as it involves determining not just the cost of power produced by the generators but also the operational status of each generation unit.

Characteristics of the generating sets such as the ramp rates, cold start costs, and cold start hours collectively affect the decision to shut down or start up a generating unit, and these are considered in the modeling of the generation dispatch controls. This means that the Unit commitment problem encompasses the economic dispatch problem, and it should be noted that any mention of economic dispatch in the remainder of this thesis is a part of the unit commitment problem. Illustration of the modified IEEE 24 bus system adapted from George-Williams and Patelli [31] is shown in figure 3.4 below. It is based on the IEEE reliability test system -1996 prepared by the reliability test system task force of the Application of Probability Methods Subcommittee for use in bulk power system reliability evaluation studies. It is composed of 24 buses, with 34 power lines and 10 generators. The charging stations have been randomly assigned to buses 1, 3, 15, 19 and 24 for this study.

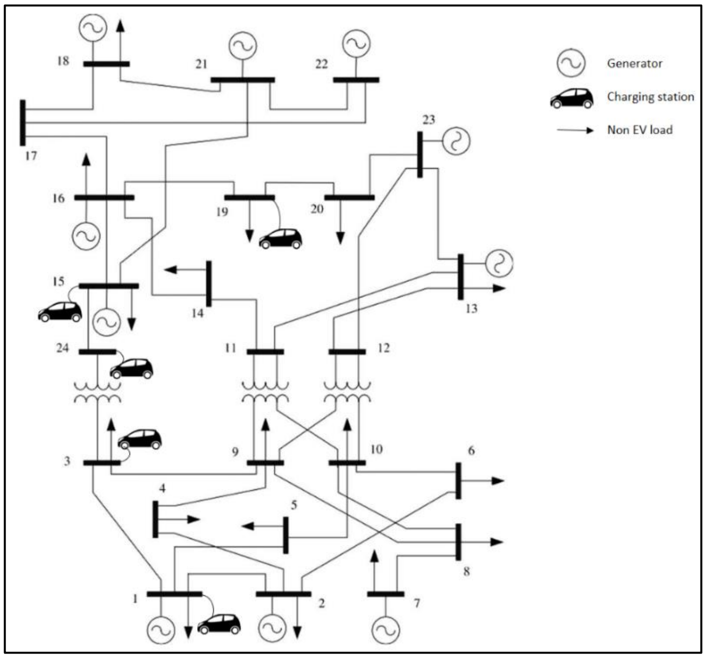

Figure 3.4 Modified IEEE 24 Bus system

It is worth noting that the following assumptions were made for the formulation of the unit commitment problem.

i.) The different charging stations communicate with one another and are under a central control that is managed by an aggregator.

ii.) PEVs are aware of their departure time, the minimum SOC of charge that they want at departure and their target SOC.

iii.) It is assumed that the different charging units are equipped with smart metering technology and can directly access the PEVs SOC. This is required to obtain the dynamic SOC of PEVs as the optimization takes place over the period.

iv.) It is assumed that this is a smart grid and that the generating units, charging stations, and the participating PEVs are in constant communication.

v.) DC power flow framework is used for modeling the power flow in the bus system. This is because the use of the AC power flow model increases the number of decision variables to be considered, which in turn leads to an increase in computational complexity.

The economic dispatch objective is shown below. The aim is to minimize the total cost needed for energy generation. Generally, the fuel costs of thermal generators in an economic dispatch problem are usually described as a quadratic function, as seen below [32].

$$F_{cost} = \sum_{g=1}^{N} agPg^2 + bgPg + cg \qquad (1)$$

Where N is the number of generating units; ag, bg, and cg are the cost coefficients of the gth generating unit, and Pg is the active output power of the generating unit. The total active power. The active output power Pg is determined by the total demand of the non PEV loads and the PEV load demand and supply. The formulation of this relationship is expressed in equation 26 where the load balance at the bus with PEVs is accounted for by the Pg, non-PEV loads and PEV loads.

Because of the quadratic nature of the economic dispatch problem, the model becomes a challenging non-linear optimization problem. Linearization of the quadratic form of the fuel cost function is suggested since this carries out the optimization faster and it is less computationally challenging to achieve results. Linearization of the fuel cost function is implemented by dividing the cost function into piece-wise linear segments. As shown in figure 3.6 below, the fuel curve between the intervals Pmin and Pmax is divided into equally sized linear intervals, which, when aggregated, are an estimate of the quadratic cost function. The precision of this linearized form can be increased by increasing the number of intervals between Pmin and Pmax [33]. The properties for the generating sets used in our study are adopted from the textbook by Soroudi [33].

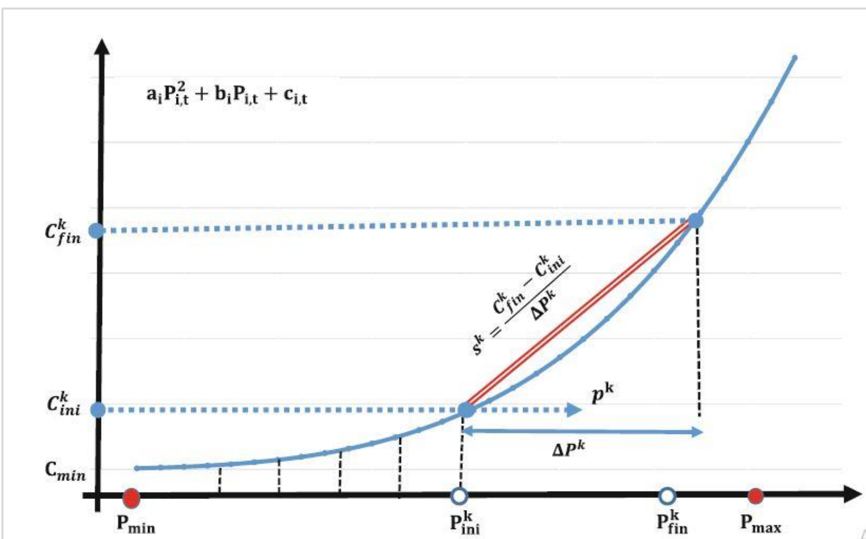

Figure 3.5 Linearization of a quadratic function [33]

The objective function to be minimized is the summation of the fuel costs, start up costs and shut down of the thermal units.

$$\text{Objective function} = \sum_{g,t} Fuel_{cost}^{g,t} + StartUp^{g,t} + ShutDown^{g,t} \qquad (2)$$

The objective function is subject to the following constraints below. Constraints shown in equations 3 to 8 account for the individual vehicle charging behaviors.

Charging or discharging only takes place when the vehicle is available in the parking lot: This constraint ensures that the charging variable is always equal to zero if the time index t for a PEV i is now between the PEV's given arrival and departure time.

$$C_{chg}^{i,t} + C_{dch}^{i,t} = 0, \forall, arr_{time}^{i} \leq t \leq dep_{time}^{i} \qquad (3)$$

Where arr_{time}^{i} and dep_{time}^{i} are the arrival and departure time of PEV i respectively.

Charging and discharging cannot take place at the same time: This constraint ensures that a vehicle does not carry out charging and discharging at the same time.

$$I_{chg}^{i,t} + I_{dch}^{i,t} \leq 1 \qquad (4)$$

Where $I_{chg}^{i,t}$ and $I_{dch}^{i,t}$ are binary variables indicating charging and discharging respectively.

Battery cap constraint: This constraint ensures that the maximum level of the SOC is set to 90% of the battery capacity to protect the battery from degradation due to overcharging.

$$soc^{i,t} \leq 0.9 * Bat_{cap}^{i} \qquad (5)$$

Where Bat_{cap}^{i} is the battery capacity for the specific vehicle i.

Minimum SOC on departure: This constraint ensures that the vehicle battery cannot be further discharged if the SOC is below the minimum required SOC.

$$I_{dch}^{i,t} = 0 \; \forall \; Msoc^{i} \geq soc^{i,t} \qquad (6)$$

Where $Msoc^i$ is the minimum desired SOC.

SOC change: This constraint shows the relationship between the SOC in the present and previous period depending on whether charging or discharging occurred.

$$soc^{i,t} = soc^{i,(t-1)} + (C_{chg}^{i,t} * \eta_{chg}) - (C_{dch}^{i,t} * \eta_{dch}) \quad (7)$$

Where η_{chg} and η_{dch} are the charging and discharging efficiencies respectively.

Total power charge: The total power charged during each period is given by

$$P_{total}^{t} = \sum_{i=1}^{I} C_{chg}^{i,t} \quad (8)$$

Generating unit lower limit: This constraint ensures that the generating unit does not operate lower than its minimum capacity.

$$P_g^{min} \leq P_{g,t} \quad (9)$$

Where P_g^{min} is the minimum operating limit of the generator.

Generating unit upper limit: This constraint ensures that the generating unit does not exceed its maximum capacity.

$$P_{g,t} \leq P_g^{max} \quad (10)$$

Where P_g^{max} is the upper operating limit of the generator.

Generator on and off state constraints: This constraint represents the relationship between on/off states, start-up and shut-down states

$$y_{g,t} - z_{g,t} = u_{g,t} - u_{g,t-1} \quad (11)$$

Where $u_{g,t}$ is a binary variable representing on and off state at 1 and 0 respectively. $y_{g,t}$ is a binary variable representing start-up state and $z_{g,t}$ is a binary variable representing the shut-down state.

Start-up and shut-down states cannot occur together: This constraint ensures that generation units cannot start up and shut down at the same hour.

$$y_{g,t} + z_{g,t} \leq 1 \tag{12}$$

Start-up cost: This calculates the cost of starting up the generator based on the start-up binary variable $y_{g,t}$. Where costST_g is the cost of starting up generator.

$$StartUp^{g,t} = y_{g,t} * \mathrm{costST}_g \tag{13}$$

Shut-down cost: This calculates the cost of shutting down the generator based on the shut-down binary $z_{g,t}$. Where costSD_g is the cost of shutting down generator.

$$ShutDown^{g,t} = z_{g,t} * \mathrm{costSD}_g \tag{14}$$

Generator minimum uptime constraints: These constraints ensure that the generating unit satisfies the minimum up-time of the unit.

$$\sum_{t=1}^{Li} 1 - u_{g,t} = 0 \; \forall \text{ g} \in \text{G}, \forall \text{ t} \in 1, \ldots\ldots \text{ Li} \tag{15}$$

Where Li is the number of periods the unit must stay on when operational. It also depends on the number of periods that the unit has been on before the first period (t = 0) of the optimization period. It is given by the expression below:

$$\text{Li} = \min \{\text{T}, (\text{minUT} - UT_{g,0}) * u_{g,0} \} \tag{16}$$

$UT_{g,0}$ is the number of periods that the generating unit has been on before the start of the optimization period.

Minimum up-time constraint for t > T – minUT + 1:

$$\sum_{t=1}^{Li} u_{g,t} - y_{g,t} \geq 0 \quad (17)$$

Where minUT is the minimum up-time constraint for the generator. This constraint ensures that any generator operational towards the end of the optimization period remains on until the minimum uptime has been reached.

Minimum up-time for t > T – minUT + 2:

$$\sum_{t=1}^{T} u_{g,t} \geq y_{g,t} * \text{minUT} \;\; \forall \text{ g} \in \text{G}, \forall \text{ t} \in 1, \ldots\ldots \text{ T} - \text{minUT} + 2 \quad (18)$$

The constraint above enforces minimum up time constraint for the last up time hours.

Generator minimum downtime constraints: These constraints ensure that the generating unit satisfies the minimum downtime of the unit.

$$\sum_{t=1}^{Fi} u_{g,t} = 0 \; \forall \text{ g} \in \text{G}, \forall \text{ t} \in 1, \ldots\ldots \text{ Fi} \quad (19)$$

Where Fi is the number of periods the unit must stay off when not in operation. It also depends on the number of periods that the unit has been off before the first period (t = 0) of the optimization period.

$$\text{Fi} = \min \{\text{T}, (\text{minDT} - DT_{g,0}) * (1 - u_{g,0})\}$$

$DT_{g,0}$ is the number of periods that the generating unit has been off before the start of the optimization period.

Minimum downtime constraint for t > T – minDT + 1:

$$\sum_{t=1}^{Fi} 1 - u_{g,t} - z_{g,t} \geq 0 \qquad (20)$$

This constraint ensures that any generator not in operation towards the end of the optimization period remains off until the minimum downtime has been reached.

Minimum downtime for t > T – minDT + 2:

$$\sum_{t=1}^{T} 1 - u_{g,t} \geq z_{g,t} * \text{minDT} \ \ \forall \text{ g} \in \text{G}, \forall \text{ t} \in 1, \ldots\ldots \text{ T} - \text{minDT} + 2 \qquad (21)$$

Shutdown limit constraints: If the unit is on at time (t-1) and turned off at time t, then the generated power at time (t-1) should be less than the shutdown limit SD. This constraint also ensures that a power drop from one period to the next does not exceed the ramp down limit.

$$P_{g,t-1} - P_{g,t} \leq u_{g,t} * RampDown_g + z_{g,t} * SD_g \ \forall \qquad (22)$$

In case of shut down in the next hour (t+1), power cannot be more than the SD limit

$$P_{g,t} \leq (u_{g,t} - z_{g,t+1}) * P_g^{max} + z_{g,t+1} * SD_g \ \forall \qquad (23)$$

If the unit has been off in the previous hour and is turned on at time t, then P cannot be more than start up limit SU. This constraint also ensures that an increase in power from one period to the other does not exceed the ramp up limit.

$$P_{g,t} \leq P_{g,t-1} + u_{g,t-1} * RampUp_g \ z_{g,t+1}) * P_g^{max} + y_{g,t} * SU_g \ \forall \qquad (24)$$

Power flow constraints: Active power flow between buses b and n for every line Ω

$$P_{nb} = \frac{\delta_n - \delta_b}{x_{nb}} \text{ nb} \in \Omega \qquad (25)$$

Where δ_n and $\delta_b$are the voltage angles for buses n and b respectively. The angle of the slack bus in this case is assumed to be zero.

Load flow balance between buses, power generated, PEV and non PEV loads

$$\sum_b P_{g,t} - Load_{b,t} - TotalEVDemand_{b,t} + TotalEVSupply_{b,t} = \sum_{nb} P_{nb} \qquad (26)$$

This ensures that the total power flow between the buses and nodes are balanced in relation to both the PEV and non-PEV loads on the bus. The scheduling of the PEVs during the optimization process occurs at the buses where the PEVs are located.

3.3 ACCOUNTING FOR BATTERY DEGRADATION

The battery remains one of the most expensive parts of an electric vehicle; therefore, it is crucial to consider the effect that cycling of the PEVs batteries to support the unit commitment problem will have on the battery life of PEVs. To account for this effect of V2G, factors such as the battery cycles and charging power are analyzed. Degradation can occur due to calendar aging and cycling aging. Calendar aging is caused by factors such as the age of the battery, and the temperature while cycling aging is caused by charging and discharging the vehicles over cycles [34]. The degradation in this thesis is focused on the cycle charging since this is the type of degradation that occurs during the V2G process due to repeated deep cycling of the battery [35].

A cycle in this study is defined as when a battery begins discharging to a certain depth of discharge and charging back to its initial SOC when the discharge cycle started. To account for the cost of degradation, the linear model by Ortega-Vazquez has been adopted. It is assumed in this formulation that the degradation curve in figure 3.7 below is for round trip cycles. A charging process of equal magnitude would occur at some point in the future for any discharging that takes place [36].

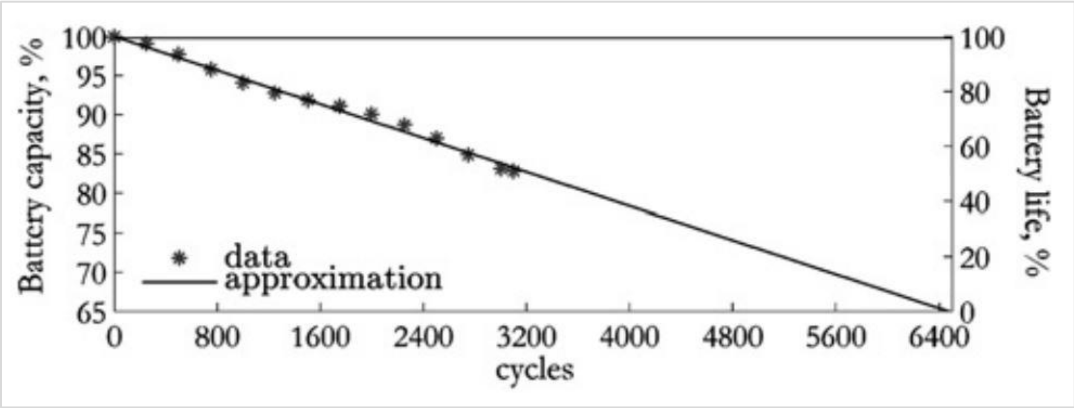

Figure 3.6 Cycle-life performance of a Nanophosphate® Li-ion battery [36]

Battery degradation constraints: The constraints below are used to account for the formulation of the cycles.

$$soc_{i,t} - soc_{i,t-1} > 0 \Leftrightarrow charge_{i,t} = 1 \;\forall \text{ i} \tag{23}$$

This constraint defines the $charge_{i,t}$ a variable that indicates when there is an increase in the SOC of the PEV.

$$soc_{i,t} - soc_{i,t-1} < 0 \Leftrightarrow discharge_{i,t} = 1 \;\forall \text{ i} \tag{24}$$

This constraint defines the $discharge_{i,t}$ variable which indicates when there is a decrease in the SOC of the PEV.

$$soc_{i,t} - soc_{i,t-1} = 0 \Leftrightarrow stable_{i,t} = 1 \;\forall \text{ i} \tag{25}$$

This constraint defines the $stable_{i,t}$ variable which indicates when neither charging nor discharging takes place.

$$charge_{i,t} + discharge_{i,t} + stable_{i,t} = 1 \;\forall \text{ i} \tag{26}$$

This constraint ensures that neither $charge_{i,t}, discharge_{i,t}$ nor $stable_{i,t}$ occur at the same time as the other.

$$\mathrm{dis}charge_{i,t} - discharge_{i,t+1} + cstart_{i,t} - cend_{i,t} = 0 \;\forall\, \mathrm{i}, \mathrm{t} > 1 \tag{27}$$

$$cstart_{i,1} = discharge_{i,1} \;\forall\, \mathrm{i} \tag{28}$$

$$\sum_t cstart_{i,t} = \sum_t cend_{i,t} \tag{29}$$

The sum of cycles for a PEV i is given below as

$$cycle_i = \sum_t cend_{i,t} \tag{30}$$

Finally, the battery degradation cost is given as:

$$Cdeg_{i,t} = \left|\frac{k}{100}\right| * \frac{x_i}{B_i} * C_i^B \tag{31}$$

Where k represents the slope of the linear approximation of the battery life as a function of the cycles. B_i is the battery capacity, C_i^B is the battery cost, and x_i denotes the accumulated energy charged and discharged from the battery [35].

The cost of batteries used for the simulation is obtained from a study conducted the U.S. International Trade Commission (USITC) [37].

Table 3.2 Cost of batteries for Electric vehicles

Vehicle model	2017 unit sales	Battery size	Battery pack assembly	Cell manufacturing	Battery cost per vehicle ($)	Total value added ($)
Tesla Model S	27,060	75.0	United States	Japan	14,250	6,413
Tesla Model 3	1,772	50	United States	United States	9,500	4,275
Tesla Model X	21,315	75	United States	Japan	14,250	6,413

Ford Focus Electric	1,817	33.5	United States	United States	7,002	3,151
Chevy Bolt	23,297	60	United States	South Korea	12,500	5,625
Fiat 500e	5,380	24.0	United States	United States	5,016	2,257
VW e-Golf	3,534	35.8	Hungary	South Korea	7,482	3,367
BMW i3	6,276	22.0	Hungary	South Korea	4,598	2,069
Nissan Leaf	11,230	26.0	United States	United States	5,434	2,445
Kia Soul EV	2,157	27.0	South Korea	South Korea	5,643	2,539

The General Algebraic Modeling System was used alongside MATLAB for modeling the optimization problem [38]. GAMS is a high-level modeling system for solving optimization problems. Solving optimization problems using GAMS requires the use of third-party solvers such as BARON, CPLEX, Gurobi, and CONOPT. CPLEX was selected as the choice solver for our study because of its capability of solving linear, quadratically constrained, and mixed-integer programming problems quickly and efficiently [38]. MATLAB was used in this research for data management and displaying of the results of the optimization.

CHAPTER 4

RESULTS

In this chapter, the results of the model presented in the previous chapter are discussed. Different scenarios are presented to show the results of the V2G system with varying levels of penetration of electric vehicles. A scenario with no control or optimization applied is also displayed, and comparison is made between it and results that include optimization.

4.1 RESULTS FOR 100,000 VEHICLES IN A SYSTEM WITHOUT V2G

The first scenario that has been simulated shows the result for 100,000 vehicles in a system with no V2G implemented. This means that on arrival at a charging station, the vehicles plug in and charge to their desired SOC without any form of scheduling, such as delayed charging. The data information for ten generating units used in the simulation is given in Appendix A. Figure 4.1 below shows the behavior of generators for the system without V2G scheduling.

From figure 4.1 it can be seen that the generators carry out unit commitment to minimize the cost of power for supplying both the PEV loads and non-PEV loads. In this case, scheduling or controlled charging of the PEVs does not occur. Generator 4 which has the smallest operating cost is seen to operate at full capacity compared to other generators such as generators 2, 9, and 10 that have high operating costs. Generators 2, 6, and 9 remain mostly in a shutdown state to minimize the cost of generation. It can also be seen that the generators stayed within their ramp rate constraints while ramping up or down. Generators can also be observed to remain within their maximum and minimum power capacity. The total cost of operating the thermal generators for a system with unit commitment and 100,000 vehicles without V2G is **$427,070.89.**

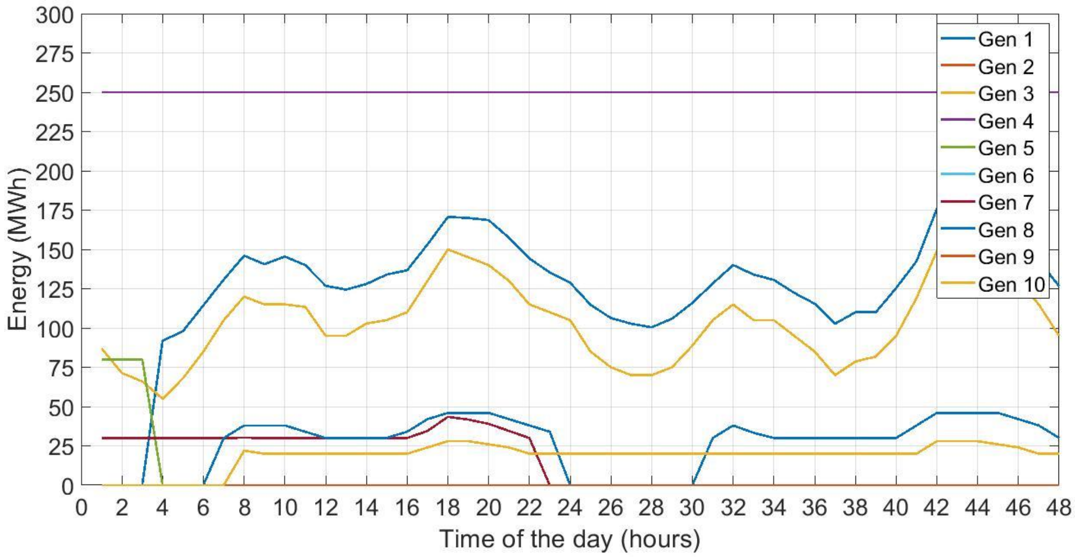

Figure 4.1 Energy supplied by generators for system without V2G

Figure 4.2 below shows the charging pattern of the PEVs at different periods of the day. As illustrated, no discharging occurs for the uncontrolled charging scenario since discharging is a function of the bidirectional V2G. The charging patterns of the PEVs are not affected by the total non-PEV load demand in an uncontrolled scenario. A closer look at the total energy generated curve, and the total non-PEV load demand curve shows that no peak shaving or valley filling occurs.

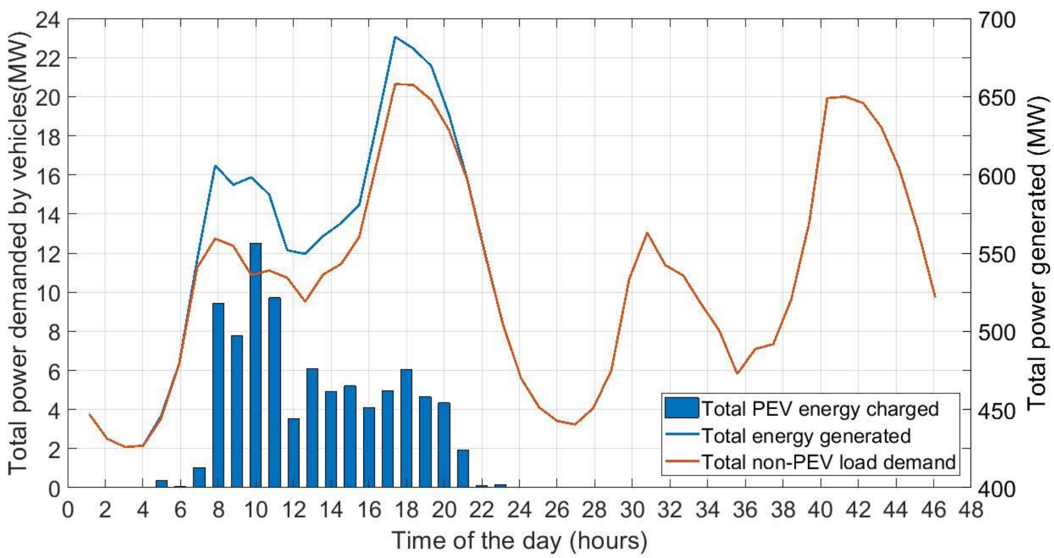

Figure 4.2 Profile of generation and PEV for 100,000 vehicles without V2G

Another point worth noting is that although calendar degradation occurs during the charging process, no cycling degradation occurs for the case without V2G.

4.2 RESULTS FOR 100,000 VEHICLES IN A SYSTEM WITH V2G

Figure 4.3 below shows the result for the simulation of 100,000 vehicles in the system. As illustrated, the unit commitment behavior of the generators is similar to the previous case in a system without V2G. Generator 4 which has the least operating cost also operates at full capacity compared to other generators. The difference in this case with V2G however can be observed in the flatter profiles of the generators. This is due to the use of PEVs in the system. The total cost of operating the thermal generators for a system with unit commitment and 100,000 vehicles not just acting as additional weight but providing V2G services was calculated as **$426,922.29.** When compared to the system with no V2G applied, solving the unit commitment problem with V2G has no significant reduction on the operation cost of the thermal units.

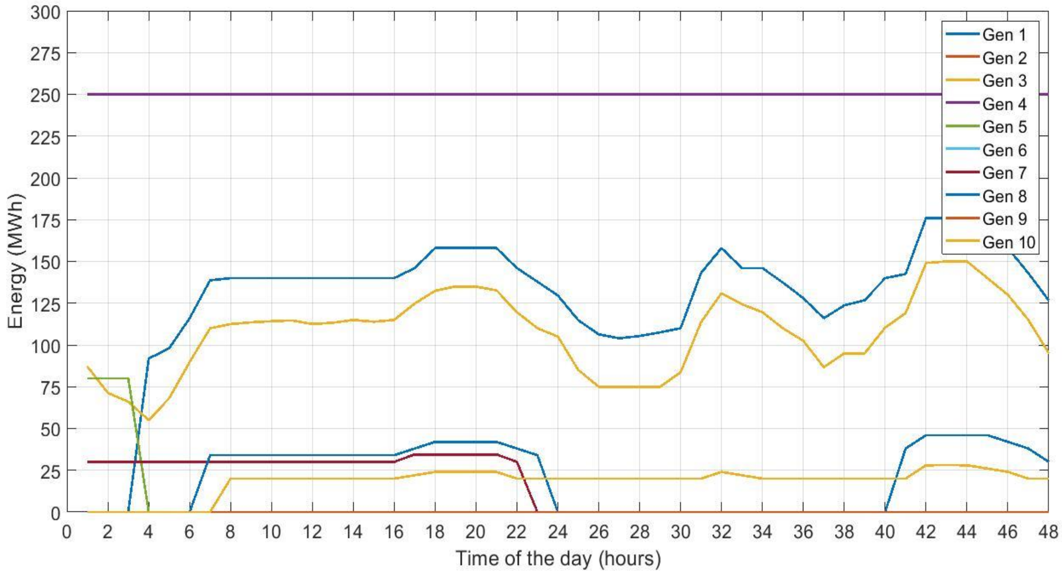

Figure 4.3 Energy supplied by generators for system with V2G.

In figure 4.4, the total energy generated, and the total non-EV load in the system are presented. These are also compared to the total energy charged and discharged by the PEVs in the system. It can be observed that for most of the period where there was not a lot of PEV load in the system, the power generated matched the total non- PEV load demand based on the system's non-EV load profile. When the number of PEVs in the system increases, starting at about hour 7, power generated becomes steadier and flatter. This behavior is due to the PEV batteries playing a significant role in reducing the need for generators to ramp up or ramp down, which reduces the cost of operation of the generators. It can also be observed that between hours 12 and 22, there is an increase in the amount of power discharged by the PEVs. This is because of the V2G process where the vehicles carry out discharging to support the grid during periods of peak non-EV load demand.

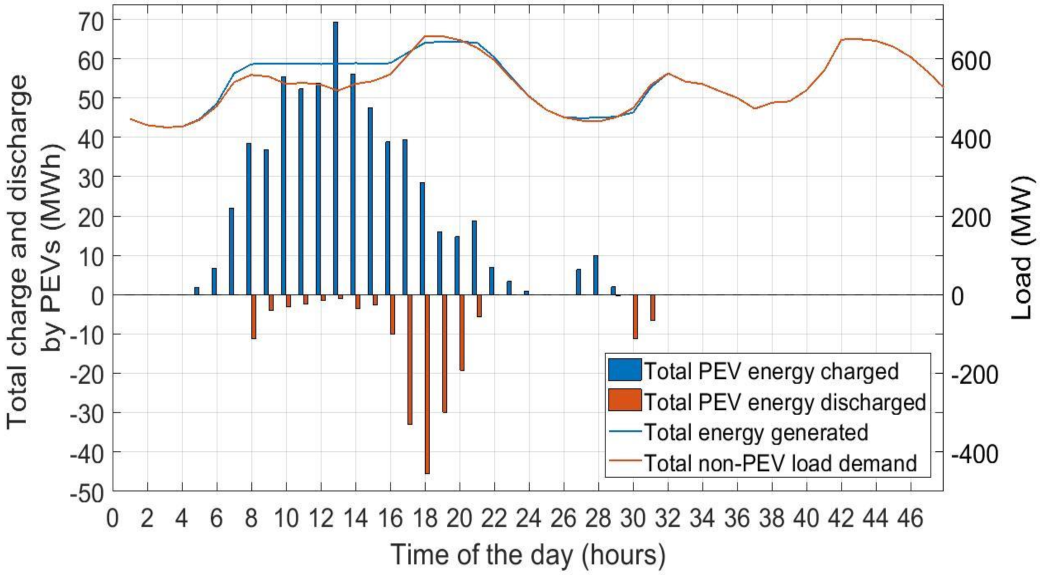

Figure 4.4 Profile of generation and PEV for 100,000 vehicles with V2G

Figure 4.5 shows the degradation cost of PEVs participating in solving the unit commitment problem. The degradation cost was based on the model introduced in the methodology chapter and takes into account the cost of the battery and the amount of cycling that takes place during V2G. As seen in the figure below, cycling degradation, which is considered in this thesis, occurs only in cases where there is discharging in the case of bidirectional V2G. An increase in the degradation cost is seen in periods where there is a high occurrence of discharging. For a simulation with 100,000 vehicles, the total cost of battery degradation is given as **$13,666.80**. The total number of cycles for 100,000 vehicles was also found to be **63,700**.

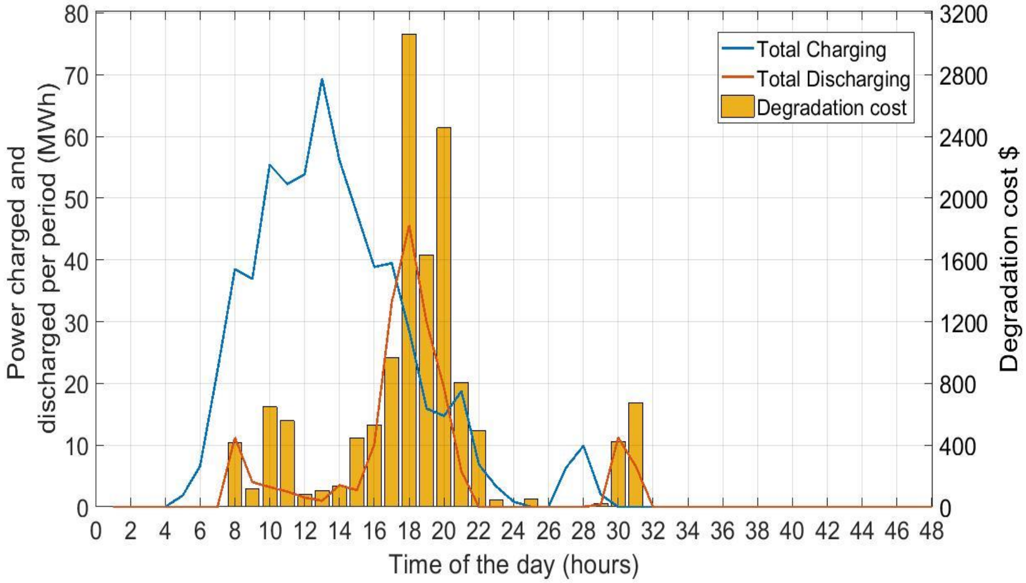

Figure 4.5 Degradation cost of PEVs in system

The cost per unit energy in the different cases were also accounted for. Cost per unit energy is the total cost of generation which is the operation cost including the respective start-up and shut down costs of the generators divided by the total power produced by generators. Figure 4.6 below shows the cost per unit energy for the different scenarios. The average cost per unit energy of the uncontrolled case was given as $16.38 per MWh while that of the controlled case with V2G was given as $16.37 per MWh. This is a very minimal reduction of the cost per energy generated. Showing that V2G is not very efficient in reduction of the generation cost of power systems with large thermal power generators but instead performs better in load leveling services.

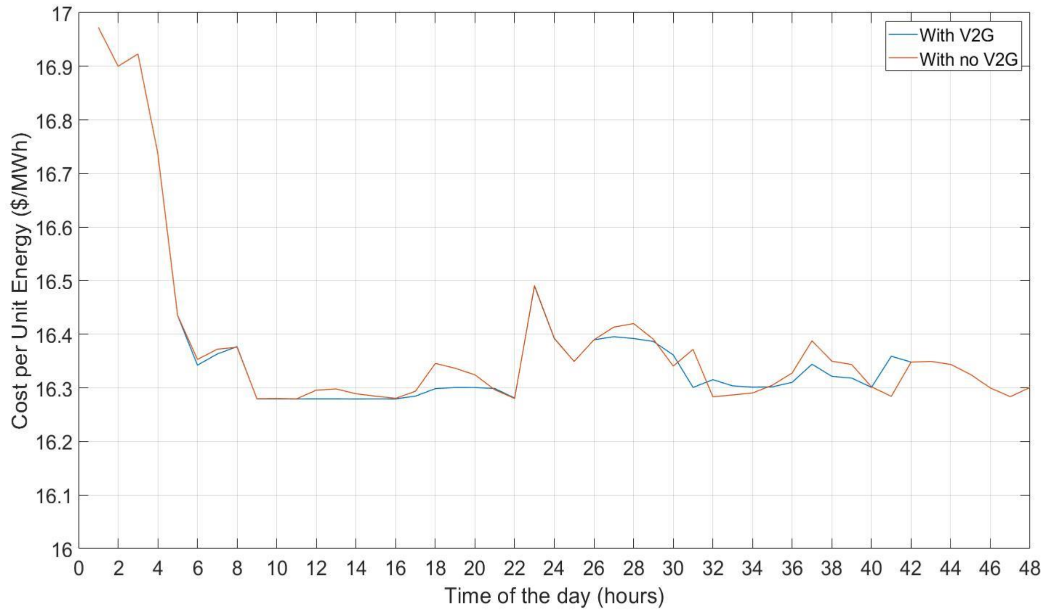

Figure 4.6 Cost per unit energy for both cases with and without V2G

4.3 DISCUSSION:

In this section, the cost-benefit analysis of employing V2G in solving the unit commitment problem is discussed. The total cost of thermal units in operation is used as an indication of economic feasibility. To check the sensitivity of the model to changes in parameters of the system, the penetration level is analyzed to determine how much an increase in the number of vehicles participating in V2G in the system can affect the quality of the power grid and economic feasibility.

Table 4.2: Results of different penetration levels

Scenario	Operation cost	Battery degradation	Number of cycles	Average cost per unit energy
Uncontrolled 100,000 vehicles	$427,070.89	0	0	$16.38
Controlled 100,000 vehicles	$426,922.27	$13,666.80	63,700	$16.37
Uncontrolled 200,000 vehicles	$432,782.31	0	0	$16.38
Controlled 200,000 vehicles	$432,635.44	$24,936.52	101,400	$16.37
Uncontrolled 500,000	$459,968.70	0	0	$16.39
Controlled 500,000 vehicles	$459,630.60	$62,666.04	147,500	$16.38

Uncontrolled 1,000,000	$504,505.55	0	0	$16.43
Controlled 1,000,000 vehicles	$503,579.86	$123,854.86	171,000	$16.41

From the table above, results show that the use of V2G for smart charging did not result in significant reductions in the system thermal generation cost. An increase in the number of vehicles in the system led to a rise in the cost of generation, which is expected. For a more detailed analysis, the cost of generation is normalized with respect to the amount of power generated. The normalized average cost per unit energy does not also display a significant difference between the cases with and without V2G.

The cost of degradation when considered at the different penetration levels has a significant impact on the economic feasibility of V2G for solving unit commitment. Increasing the number of vehicles participating in V2G resulted in a rise in the degradation costs as more vehicles carry out cycling. Although the use of V2G to solve the unit commitment does not result in a significant reduction of generation cost, V2G is very useful in flattening the load profile, and this is an ancillary service that is useful in power systems that face the risk of line congestions. By delaying charging of PEVs to periods of lesser congestions or power demand, V2G can result in valley filling and peak shaving of the power profile as shown in Figure 4.7 below. shows the load profiles for the systems with and without V2G applied.

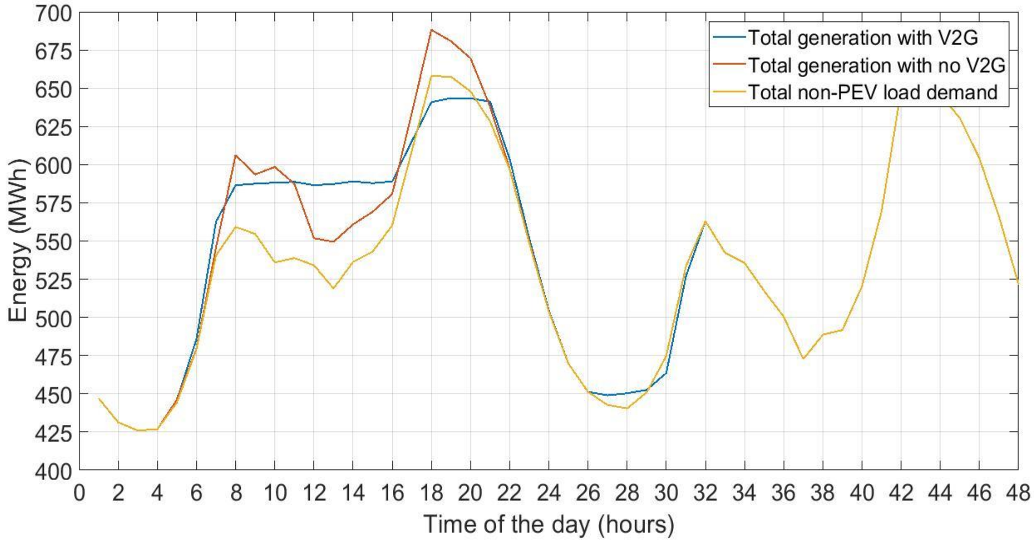

Figure 4.7 Load profiles for system with V2G and without V2G

CHAPTER 5

CONCLUSION

In this thesis, a unit commitment model with V2G was presented. The model was tested on an IEEE 24 bus system by implementing several scenarios. In the first scenario, the system was simulated without the use of V2G to solve the unit commitment problem. Results show that the application of V2G led to battery degradation due to the use of vehicle batteries for cycling. Battery degradation therefore is a major challenge to V2G being used for the unit commitment problem. Although the use of V2G did not result in a significant reduction in the thermal generation cost, PEVs in the system resulted in a flatter load profile which is desirable for the power system. This ancillary service can be very useful in systems that are prone to congestions or overloading. Coordinating V2G with renewable energy integration will result in an even more economical system. The battery of the PEVs will be useful as a reservoir to store renewable energy during periods of excess generation for use in periods when the renewable energy is not operational. This will result in a lighter burden on the thermal units.

5.1 FUTURE WORK:

1.) Analyses of emissions cost from the use of thermal generators can be evaluated in future work. This will require the emissions data of the specific generators used in the system. The emissions and cost objectives that might be conflicting will be accounted for as multi-objective scenarios.

2.) Transmission losses in both lines and transformers can be included in the optimal power flow and cost calculation in the system.

3.) Online scheduling of the model can be implemented for cases where the load demand of the non-EV loads and the duration of the PEVs at the charging stations cannot be accurately forecasted ahead of the optimization

REFERENCES

1. Irle, R. Global EV Sales for the 1st Half of 2019. 2019; Available from: http://www.ev-volumes.com/country/total-world-plug-in-vehicle-volumes/.
2. Hertzke, P., et al. Expanding electric-vehicle adoption despite early growing pains. 2019 [cited 2020 January 20]; Available from: https://www.mckinsey.com/industries/automotive-and-assembly/our-insights/expanding-electric-vehicle-adoption-despite-early-growing-pains.
3. Ascher, D. and G. Hackenberg. Integrated transportation and power system modeling. in 2015 International Conference on Connected Vehicles and Expo (ICCVE). 2015.
4. Kempton, W. and J. Tomić, Vehicle-to-grid power fundamentals: Calculating capacity and net revenue. Journal of Power Sources, 2005. **144**(1): p. 268-279.
5. Melaina, M. and M. Penev, Hydrogen Station Cost Estimates. 2013, National Renewable Energy Laboratory.
6. Kisacikoglu, M.C., et al., PHEV-EV charger technology assessment with an emphasis on V2G operation. Oak Ridge Nat. Lab., Oak Ridge, TN, USA, Tech. Rep. ORNL/TM-2010/221, 2012.
7. Gong, X. and J. Rangaraju, Taking charge of electric vehicles-both in the vehicle and on the grid. Texas Instruments, Dallas, TX, USA, 2018: p. 1-13.
8. NREL. Connecting Electric Vehicles to the Grid for Greater Infrastructure Resilience. 2017 [cited 2020 January 20]; Available from: https://www.nrel.gov/news/program/2017/connecting-electric-vehicles-to-the-grid-for-greater-infrastructure-resilience.html.
9. Sortomme, E. and M.A. El-Sharkawi, Optimal Charging Strategies for Unidirectional Vehicle-to-Grid. IEEE Transactions on Smart Grid, 2011. **2**(1): p. 131-138.
10. Sekyung, H., H. Soohee, and K. Sezaki, Development of an Optimal Vehicle-to-Grid Aggregator for Frequency Regulation. IEEE Transactions on Smart Grid, 2010. **1**(1): p. 65-72.
11. Wang, B., R. Yin, and D. Black, Comprehensive Modeling of Electric Vehicles in California Demand Response Markets. arXiv.org, 2018.
12. Kisacikoglu, M.C., B. Ozpineci, and L.M. Tolbert, EV/PHEV bidirectional charger assessment for V2G reactive power operation. IEEE Transactions on Power Electronics, 2013. **28**(12): p. 5717-5727.
13. Sami, I., et al. A Bidirectional Interactive Electric Vehicles Operation Modes: Vehicle-to-Grid (V2G) and Grid-to-Vehicle (G2V) Variations Within Smart Grid. in 2019 International Conference on Engineering and Emerging Technologies (ICEET). 2019. IEEE.

14. Tan, K.M., V.K. Ramachandaramurthy, and J.Y. Yong, Integration of electric vehicles in smart grid: A review on vehicle to grid technologies and optimization techniques. Renewable and Sustainable Energy Reviews, 2016. **53**: p. 720-732.
15. Hashemi, S., et al. Frequency Regulation Provision Using Cross-Brand Bidirectional V2G-Enabled Electric Vehicles. in 2018 IEEE International Conference on Smart Energy Grid Engineering (SEGE). 2018. IEEE.
16. Hajizadeh, A. and M.R. Kikhavani, Coordination of bidirectional charging for plug-in electric vehicles in smart distribution systems. Electrical Engineering, 2018. **100**(2): p. 1085-1096.
17. Huang, Z., B. Fang, and J. Deng, Multi-objective optimization strategy for distribution network considering V2G-enabled electric vehicles in building integrated energy system. Protection and Control of Modern Power Systems, 2020. **5**(1): p. 7.
18. Bitencourt, L.d.A., et al. Optimal EV charging and discharging control considering dynamic pricing. in 2017 IEEE Manchester PowerTech. 2017. IEEE.
19. Hosseini Imani, M., et al., Impact evaluation of electric vehicle parking on solving security-constrained unit commitment problem. Mathematical and Computational Applications, 2018. **23**(1): p. 13.
20. Pan, A., et al. Stochastic Security Constraint Unit Commitment Considering the Correlation of Electric Vehicles' Driving. in 2019 IEEE Innovative Smart Grid Technologies-Asia (ISGT Asia). 2019. IEEE.
21. Sadeghian, H. and Z. Wang. Combined heat and power unit commitment with smart parking lots of plug-in electric vehicles. in 2017 North American Power Symposium (NAPS). 2017. IEEE.
22. Cao, H. and Q. Zhao. A Novel Game-Theoretic-based Security-Constrained Unit Commitment Including Wind and Vehicle-to-Grid. in 2019 Chinese Control And Decision Conference (CCDC). 2019. IEEE.
23. Yang, Z., et al., A binary symmetric based hybrid meta-heuristic method for solving mixed integer unit commitment problem integrating with significant plug-in electric vehicles. Energy, 2019. **170**: p. 889-905.
24. Azari, A.N., et al., Optimal Transmission Congestion Management with V2G in Smart Grid. American Journal of Electrical Power and Energy Systems, 2018. **7**(2): p. 16-24.
25. Kumar, A., V. Bhalla, and P. Kumar. Unit commitment in a smart grid with plug-in hybrid electric vehicles—A cost-emission optimization. in 2017 IEEE Transportation Electrification Conference (ITEC-India). 2017. IEEE.
26. Liu, H., et al. Multi-objective security-constrained unit commitment model considering wind power and EVs. in 2016 Chinese Control and Decision Conference (CCDC). 2016. IEEE.
27. Maghsudlu, S. and S. Mohammadi, Optimal scheduled unit commitment considering suitable power of electric vehicle and photovoltaic uncertainty. Journal of Renewable and Sustainable Energy, 2018. **10**(4): p. 043705.
28. Marmaras, C., E. Xydas, and L. Cipcigan, Simulation of electric vehicle driver behaviour in road transport and electric power networks. Transportation Research Part C: Emerging Technologies, 2017. **80**: p. 239-256.

29. D.O.E. The official U.S government source for fuel economy information. 2020 [cited 2019 August 20]; Available from: www.fueleconomy.gov
30. NHTS. National Household Travel Survey. 2018; Available from: https://nhts.ornl.gov/.
31. George-Williams, H. and E. Patelli, Maintenance strategy optimization for complex power systems susceptible to maintenance delays and operational dynamics. IEEE Transactions on Reliability, 2017. **66**(4): p. 1309-1330.
32. Liang, H., et al., Dynamic Economic/Emission Dispatch Including PEVs for Peak Shaving and Valley Filling. IEEE Transactions on Industrial Electronics, 2019. **66**(4): p. 2880-2890.
33. Soroudi, A., Power System Optimization Modeling in GAMS. 2017: Springer.
34. Saldaña, G., et al., Electric Vehicle into the Grid: Charging Methodologies Aimed at Providing Ancillary Services Considering Battery Degradation. Energies, 2019. **12**(12).
35. Liu, K., et al., Optimal operation strategy for distributed battery aggregator providing energy and ancillary services. Journal of Modern Power Systems and Clean Energy, 2018. **6**(4): p. 722-732.
36. Ortega-Vazquez, M.A., Optimal scheduling of electric vehicle charging and vehicle-to-grid services at household level including battery degradation and price uncertainty. IET Generation, Transmission & Distribution, 2014. **8**(6): p. 1007-1016.
37. Coffin, D. and J. Horowitz, The Supply Chain for Electric Vehicle Batteries. Journal of International Commerce and Economics, 2018.
38. GAMS. CPLEX 12. 2020 [cited 2020 January 20]; Available from: https://www.gams.com/latest/docs/S_CPLEX.html.

APPENDIX A

Table A.1 Unit commitment data for 10 thermal units [33]

Unit	ai (\$/MW^2)	bi (\$/MW)	ci (\$)	Cdi (\$)	Csi (\$)	RUi (MW h^{-1})	RDi (MW h^{-1})	UTi (h)	DTi (h)	SDi (MW h^{-1})	SUi (MW h^{-1})	Pmini (MW)	PmaxI (MW)	U1 (h)	Ui,t = 0	Si(h)
G1	0.0148	12.1	82	42.6	42.6	40	40	3	2	90	110	80	200	1	0	1
G2	0.0289	12.6	49	50.6	50.6	64	64	4	2	130	140	120	320	2	0	0
G3	0.0135	13.2	100	57.1	57.1	30	30	3	2	70	80	50	150	3	0	3
G4	0.0127	13.9	105	47.1	47.9	104	104	5	3	240	250	250	520	1	1	0
G5	0.0261	13.5	72	56.6	56.9	56	56	4	2	110	130	80	280	1	1	0
G6	0.0212	15.4	29	141.5	142	30	30	3	2	60	80	50	150	0	0	0
G7	0.0382	14	32	113.5	114	24	24	3	2	50	60	30	120	0	1	0
G8	0.0393	13.5	40	42.6	42.6	22	22	3	2	45	55	30	110	0	0	0
G9	0.0396	15	25	50.6	50.6	16	16	0	0	35	45	20	80	0	0	0
G10	0.051	14.3	15	57.1	57.1	12	12	0	0	30	40	20	60	0	0	0